*Anal. Chem.* **2002,** *74,* 2416−2422

# Ion Channel Mimetic Micropore and Nanotube Membrane Sensors

Erich D. Steinle, David T. Mitchell, Marc Wirtz, Sang Bok Lee, Vaneica Y. Young, and Charles R. Martin*

*Department of Chemistry and Center for Research at the Bio/Nano Interface, University of Florida, Gainesville, Florida 32611-7200*

**This paper describes synthetic micropore and nanotube membranes that mimic the function of a ligand-gated ion channel; that is, these membranes can be switched from an "off" state (no or low ion current through the membrane) to an "on" state (higher ion current) in response to the presence of a chemical stimulus. Ion channel mimics based on both microporous alumina and Au nanotube membranes were investigated. The off state was obtained by making the membranes hydrophobic by chemisorbing either a $C_{18}$ silane (alumina membrane) or a $C_{18}$ thiol (Au nanotube membrane). Water and electrolyte are forbidden from entering these very hydrophobic pores/nanotubes. The transition to the on state was induced by the partitioning of a hydrophobic ionic species (e.g., a drug or a surfactant) into the membrane. The membrane switches to the on state because at a sufficiently high concentration of this ionic analyte species, the pores/nanotubes flood with water and electrolyte. A pH-responsive membrane was also prepared by attaching a hydrophobic alkyl carboxylic acid silane to the alumina membrane.**

We have been exploring the transport and electrochemical properties of nanotube membranes[1−11] prepared by the template method,[12−14] a general approach for preparing nanomaterials. One possible application for these nanotube membranes is in electroanalytical chemistry in which the membrane is used to sense analyte species.[3] In our prior work, membranes containing gold nanotubes with inside diameters that approached molecular dimensions (1 nm to 4 nm) were used.[3] The Au nanotube membrane was placed between two salt solutions, and a constant transmembrane potential was applied. The resulting transmembrane current, associated with migration of ions through the nanotubes, was measured. When an analyte molecule with a diameter comparable to the inside diameter of the nanotubes was added to one salt solution, this molecule partitioned into the nanotubes and partially occluded the pathway for ion transport. This resulted in a decrease in the transmembrane ion current, and the magnitude of the drop in current was found to be proportional to the concentration of the analyte.[3]

In the experiment discussed above, a baseline transmembrane ion current was established, and the analyte molecule, in essence, turned off this current. It occurred to us that there might be an advantage in doing the opposite, that is, starting with an ideally zero current situation and having the analyte molecule switch on the ion current. That is, we would like to make a synthetic membrane that mimics the function of a ligand-gated ion channel. An example is the acetylcholine-gated ion channel,[15] which is closed ("off" state) in the absence of acetylcholine but opens (and supports an ion current, "on" state) when acetylcholine binds to the channel. This concept of ion-channel mimetic sensing, originally proposed by Umezawa's group,[16] has been of considerable interest in analytical chemistry.[17−19] There is also considerable interest in using naturally occurring and genetically engineered protein channels as sensors (see ref 20 and references therein).

We describe here the results of experiments that provide proof of the basic concept that an analyte molecule can switch on an ion current in a synthetic membrane-based ion-channel mimic. The membrane used for most experiments was a commercially available microporous alumina filter. The pores in this membrane were made hydrophobic by reaction with an 18-carbon ($C_{18}$) alkyl silane. When placed between two salt solutions, the pores in this $C_{18}$-derivatized membrane are not wetted by water, yielding the off state of the membrane. When exposed to a solution containing

* Corresponding author. E-mail: crmartin@chem.ufl.edu.

(1) Jirage, K. B.; Hulteen, J. C.; Martin, C. R. *Science* **1997**, *278*, 655−658.
(2) Hulteen, J. C.; Jirage, K. B.; Martin, C. R. *J. Am. Chem. Soc.* **1998**, *120*, 6603−6604.
(3) Kobayashi, Y.; Martin, C. R. *Anal. Chem.* **1999**, *71*, 3665−3672.
(4) Jirage, K. B.; Hulteen, J. C.; Martin, C. R. *Anal. Chem.* **1999**, *71*, 4913−4918.
(5) Lee, S. B.; Martin, C. R. *Anal. Chem.* **2001**, *73*, 768−775.
(6) Martin, C. R.; Nishizawa, M.; Jirage, K. B.; Kang, M. *J. Phys. Chem. B* **2001**, *105*, 1925−1934.
(7) Che, G.; Lakshmi, B. B.; Fisher, E. R.; Martin, C. R. *Nature* **1998**, *393*, 346−349.
(8) Che, G.; Miller, S. A.; Fisher, E. R.; Martin, C. R. *Anal. Chem.* **1999**, *71*, 3187−3191.
(9) Che, G.; Lakshmi, B. B.; Martin, C. R.; Fisher, E. R. *Langmuir* **1999**, *15*, 750−758.
(10) Nishizawa, M.; Menon, V. P.; Martin, C. R. *Science* **1995**, *268*, 700−702.
(11) Kang, M.; Martin, C. R. *Langmuir* **2001**, *17*, 2753−2759.
(12) Martin, C. R. *Science* **1994**, *266*, 1961−1966.
(13) Martin, C. R.; Mitchell, D. T. *Anal. Chem.* **1998**, *70*, 322A−327A.
(14) Hulteen, J. C.; Martin, C. R. *J. Mater. Chem.* **1997**, *7*, 1075−1087.
(15) Voet, D.; Voet, J. G. *Biochemistry*, 2nd ed.; John Wiley and Sons: New York, 1995.
(16) Sugawara, M.; Kojima, K.; Sazawa, H.; Umezawa, Y. *Anal. Chem.* **1987**, *59*, 2842−2846.
(17) Xiao, K. P.; Bühlmann, P.; Umezawa, Y. *Anal. Chem.* **1999**, *71*, 1183−1187.
(18) Wu, Z.; Tang, J.; Cheng, Z.; Yang, X.; Wang, E. *Anal. Chem.* **2000**, *72*, 6030−6033.
(19) Katayama, Y.; Ohuchi, Y.; Higashi, H.; Kudo, Y.; Maeda, M. *Anal. Chem.* **2000**, *72*, 4671−4674.
(20) Bayley, H.; Martin, C. R. *Chem. Rev.* **2000**, *100*, 2575−2594.



10.1021/ac020024j CCC: $22.00 
Published on Web 04/19/2002

a sufficiently high concentration of a long chain ionic surfactant (the analyte), the surfactant molecules partition into the hydrophobic membrane and ultimately cause the pores to flood with water and electrolyte. As a result, the membrane will now support an ion current, and the ion channel-mimetic membrane is switched to its on state. Cationic drug molecules can also switch this membrane from the off to the on state. Furthermore, when a hydrophobic −COOH-containing silane is used, the off/on transition can be induced by controlling the pH of the contacting solution phases. This analyte-induced switching of the membrane between the off and on states was investigated using an AC impedance method, transport methods, and by direct measurements of the transmembrane ion current.

## EXPERIMENTAL SECTION

**Materials.** Tris (2,2′-bipyridyl)ruthenium(II) ($Ru(bpy)_3^{2+}$) dichloride, 1,5-naphthalene disulfonic acid tetrahydrate, octadecyltrimethoxysilane, 1-dodecanesulfonic acid, 1-hexadecanesulfonic acid, 1-octanesulfonic acid, 4-octylbenzensulfonic acid, 1-propanesulfonic acid, and ethanesulfonic acid were obtained from Aldrich and used as received. Tetradecylammonium bromide was obtained from ICN Biomedicals. Hexadecyltrimethylammonium chloride, decyltrimethylammonium chloride, dodecyltrimethylammonium chloride, and dodecylbenzenesulfonic acid were obtained from Acros Chemicals. Octadecyl thiol was obtained from Aldrich. The alumina membranes were Anopore (Whatman Inc., Clifton, NJ) that had nominally 200-nm-diameter pores and were 60 $\mu$m thick. Microporous track-etched polycarbonate membranes (Osmonics) were also investigated. These membranes have 30-nm-diameter pores and a pore density of $6 \times 10^8$ $cm^{-2}$. The hydrochlorides of three cationic drug molecules—amiodarone, bupivacaine, and amytriptyline (Sigma)—were investigated as part of this work. Amiodarone is an antiarrhythmic and antianginal, bupivacaine is a local anesthetic, and amytriptyline is a tricyclic antidepressant. Their chemical structures will be discussed below.

**Membrane Preparation.** A solution that was 5% (v/v) in octadecyltrimethoxysilane was prepared in ethanol; to this solution was added acetate buffer (0.1 M, pH = 5.1) to make the solution 5% (v/v) in this buffer. The resulting solution was stirred for 5 min, and the alumina membrane was then immersed. After 2 h, the membrane was removed from the solution, rinsed with ethanol, and cured at 150 °C in air for 20 min.

Alumina membranes were also derivatized with a silane that terminated with the 20-carbon carboxylic acid $-(CH_2)_{20}-COOH$. A two-step method based on a literature procedure was used.[21,22] First, the alumina membrane was modified with an aminopropylsilane. This was accomplished by immersing the membrane into a solution prepared by mixing 2 mL of aminopropyl trimethoxysilane with 15 mL of ethanol that contained 1 mL of sodium acetate solution (50 mM, pH = 5.1). The silanization reaction was terminated after 20 min by rinsing the membrane with ethanol. The membrane was then cured in an oven at 150 °C for 1 h. The terminal amino group was then reacted with one end of the diacid chloride of $HOOC-(CH_2)_{20}-COOH$. This was accomplished by immersing the membrane into 30 mL of a dichloromethane solution that contained 100 mmol of the diacid chloride plus 10 mmol of diisopropylethylamine; the membrane was immersed for 24 h under an Ar atmosphere. The membrane was then rinsed with dichloromethane and immersed into 50 mL of aqueous acetone (10% water) for 6 h. The membrane was further rinsed with deionized water and dried in an oven at 150 °C for 1 h. The diacid chloride was prepared by treating the dicarboxylic acid with thionyl chloride.

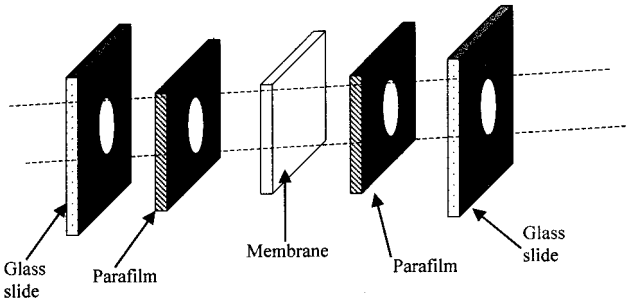

Figure 1. Membrane assembly.

Following attachment of the desired silane, the membrane was mounted into the assembly device shown in Figure 1. After assembling the various components, the assembly was heated for three minutes at 150 °C in an oven to melt the Parafilm, which acted as a glue to hold the various pieces together. This assembly exposes 0.079 $cm^2$ of membrane area to the contacting electrolyte solutions.

We also conducted a limited number of experiments with gold nanotube membranes prepared by electroless deposition of Au within the pores of the microporous track-etched polycarbonate membrane.[4] These membranes have been discussed in detail in our previous publications.[1−6,10,11] The electroless plating procedure has been previously described;[4] membranes containing Au nanotubes with inside diameters of ∼2 nm were used. The Au nanotubes were rendered hydrophobic by chemisorbing octadecylthiol to the nanotube walls.[4]

**AC Impedance Measurements.** The membrane assembly was mounted between the halves of a U-tube permeation cell, and both half-cells were filled with ∼20 mL of 0.1 M KCl. A Ag/AgCl working electrode was immersed into one half-cell solution, and a Pt counter electrode and a Ag/AgCl reference electrode were placed in the other half-cell.[23−25] Impedance data were obtained using a Solartron 1287 electrochemical interface module (Solartron Analytical, Hampshire, England) connected to a Solartron 1255B frequency response analyzer and a personal computer. The magnitude of the sinusoidal potential perturbation applied across the membrane was ±20 mV; impedance data were obtained over a frequency range of $10^6$−0.1 Hz. Z-plot and Z-view software packages (Scribner Associates, Inc., Southern Pines, North Carolina) were used to control the impedance experiments and analyze the impedance data.

**X-ray Photoelectron Spectroscopy (XPS).** XPS was used to show that the prototypical analyte dodecylbenzene sulfonate (DBS) is present on the $C_{18}$-modified alumina surface after exposure of the membrane to DBS solution. However, the XPS cross section for S from the DBS proved too weak to obtain

(21) Archibald, D. D.; Qadri, S. B.; Gaber, B. P. *Langmuir* **1996**, *12*, 538−546.
(22) Cohen, Y.; Levi, S.; Rubin, S.; Willner, I. *J. Electroanal. Chem.* **1996**, *417*, 65−75.
(23) Armstrong, R. D.; Covington, A. K.; Evans, G. P. *J. Electroanal. Chem.* **1983**, *159*, 33−40.
(24) Xie, S.-L.; Cammann, K. *J. Electroanal. Chem.* **1987**, *229*, 249−263.
(25) Zhang, W.; Spichiger, U. E. *Electrochemica Acta* **2000**, *45*, 2259−2266.

unambiguous evidence; furthermore, O, C, and $Na^+$ (the counterion for the DBS) are ubiquitous and, therefore, not useful as probes to prove that DBS is present on the surface. For this reason, we used a surface ion exchange reaction to replace $Na^+$ with $Cs^+$ as the counterion for the surface-bound DBS. We then used XPS to look for the presence of $Cs^+$ on the $C_{18}$-modified surface that had been treated with DBS using an identical surface that was exposed to the $Cs^+$ solution but not to DBS as the control.

A section of the $C_{18}$ membrane was immersed for 5 min into an aqueous 2.0 mM solution of $Na^+$-DBS. Following exposure to surfactant, the membrane was rinsed repeatedly with deionized water and then immersed for 5 min in a 100 mM aqueous solution of $CsNO_3$. After rinsing again with deionized water, the sample was air-dried. XPS studies were performed on a Kratos XSAM 800 spectrometer using Al $K_\alpha$ excitation (200 W). The samples were mounted onto a stainless steel sample stub by means of a 7-mm-diameter carbon sheet disk (SPI Supplies) so as to completely cover both the carbon disk and the sample stub. The samples were inserted into the sample analyzer chamber via a quick insertion probe, and spectral acquisition using the fixed analyzer transmission mode commenced after the pressure decreased to $5 \times 10^{-9}$ Torr. An incident angle of 75° relative to the sample surface was employed.

**Transport Experiments.** The membrane was mounted between the two halves of a U-tube permeation cell, and 0.1 M KCl was added to each half-cell. The feed half-cell was also 50 $\mu$M in either $Ru(bpy)_3^{2+}$ or naphthalene disulfonate ($NDS^{2-}$), the permeate ions. These permeate ions were chosen because transport from the feed solution through the membrane and into the permeate solution can be easily monitored by measuring the UV absorbance of the permeate solution. (Both permeate ions were detected at 286 nm.) Transport occurred by diffusion of the permeate ion down the concentration gradient across the membrane; both the feed and permeate half-cells were vigorously stirred during the permeation experiments.

The experimental protocol used was as follows: An increment of the analyte surfactant (for these experiments, DBS) was added to both the feed and permeate half-cells, and permeation was allowed to occur for 24 h. After this time, the permeate half-cell was sampled, and the UV absorbance was used to determine the moles of the permeate ion transported. The permeate solution was then returned to the permeate half-cell, and a second increment of DBS was added. Permeation was again allowed to occur for 24 h, and the amount of permeate ion transported was again determined. This process was repeated for various DBS concentrations over the range from $10^{-8}$ to $10^{-4}$ M.

**Ion-Current Measurements.** The membrane was mounted between the two halves of a U-tube permeation cell, and 0.1 M KCl was added to each half-cell. A Pt wire electrode was inserted into each half-cell, and the Solartron potentiostat was used to apply a constant transmembrane voltage of 1.5 V and measure the resulting transmembrane current. The current was monitored for 30 min, and then the half-cell solutions were spiked with DBS to a total concentration of $10^{-9}$ M. The current was again measured for 30 min, and the half-cells were spiked again with DBS. This process was repeated for various DBS concentrations over the range from $10^{-9}$ to $10^{-3.5}$ M.

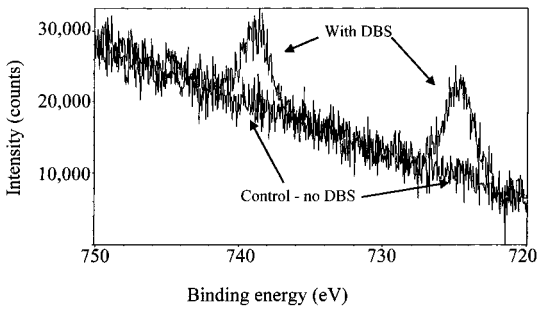


Figure 2. XPS data for a $C_{18}$-modified alumina membrane surface that was exposed to a DBS solution and then to a $Cs^+$ solution and for an identical surface that was exposed to $Cs^+$ but not to DBS.

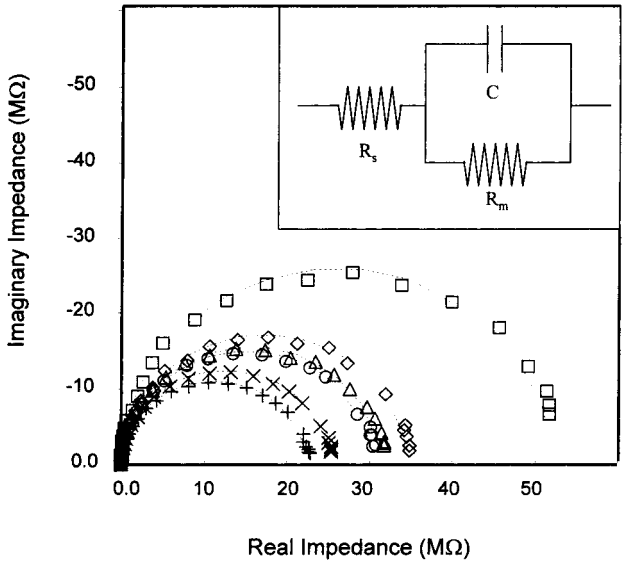


Figure 3. Nyquist plots for a $C_{18}$-modified alumina membrane upon exposure to increasing concentrations of DBS in 0.1 M KCl. The points are the experimental data. The lines are calculated data obtained using the equivalent circuit shown in the inset. Concentrations (nM) of DBS were as follows: □, 0; ♦, 1.4; △, 3; ○, 10; ×, 40; and +, 100 nM.

## RESULTS AND DISCUSSION

**XPS Studies.** We used $Cs^+$ as a probe to prove that the prototypical analyte DBS is, indeed, present on the $C_{18}$-modified alumina surface after exposure of the membrane to DBS solution. Figure 2 shows XPS data for a $C_{18}$-modified membrane that had been exposed to DBS, rinsed, exposed to $Cs^+$, and then rinsed extensively again. The Cs 3d peaks at 724 and 738 eV are clearly evident.[26] This may be contrasted to the control surface, a $C_{18}$-modified alumina membrane that was exposed to the $Cs^+$ solution but not to DBS, in which no Cs signal is seen (Figure 2). These data show that exposure of the membrane to DBS results in partitioning of this analyte species onto the $C_{18}$-modified surface.

**AC Impedance Experiments with DBS Analyte.** AC Impedance measurements proved to be a useful way to demonstrate the analyte-induced switching of the membrane between the off and on states. The upper-most curve in Figure 3 is the Nyquist plot for a $C_{18}$-modified alumina membrane with 0.1 M KCl solutions, and no DBS, on either side of the membrane. As per

(26) Muilenberg, G. E., Ed. *Handbook of X-ray Photoelectron Spectroscopy*; Perkin-Elmer Corporation: Eden Prairie, 1978.

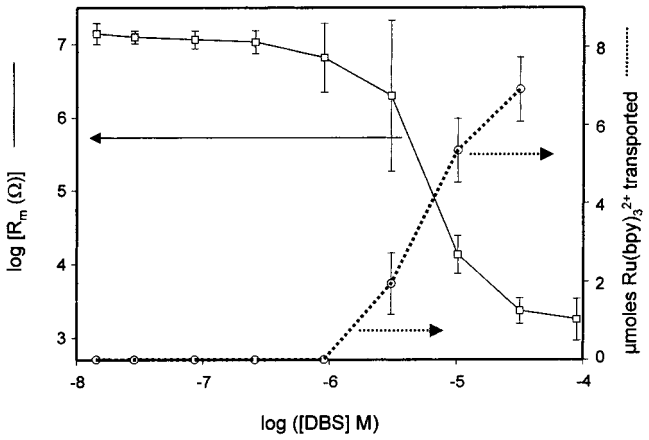


Figure 4. Plots of log membrane resistance (left *y* axis) and micromoles of $Ru(bpy)_3^{2+}$ transported across the membrane (right *y* axis) vs log[DBS] for a $C_{18}$-modified alumina membrane. The error bars represent the standard deviation of three separate experiments.

prior investigations of ion-channel and ion-channel-mimetic membranes,[27,28] the impedance data were interpreted in terms of the equivalent circuit shown in the inset of Figure 3, where $R_s$ is the solution resistance, $R_m$ is the membrane resistance, and $C$ is the membrane capacitance. The dashed curve is the best fit to the experimental data, from which the $R_m$ (Figure 4) and $C$ values were obtained. Also shown in Figure 3 are impedance data after spiking the half-cell electrolyte solutions to the indicated concentrations with the analyte DBS.

In the absence of DBS, the membrane resistance is very large, >50 MΩ as opposed to ∼5 Ω for the alumina membrane before modification with the $C_{18}$ silane. Transport experiments (vide infra) show that this is because the very hydrophobic $C_{18}$-modified pores are not wetted by water. This is supported by contact angle measurements on the membrane surface, where a water contact angle of 130 (±8)° was obtained for the $C_{18}$-treated alumina membrane, as opposed to ∼8 (±1)° for the untreated membrane. It should be noted that the contact angle for the $C_{18}$-treated alumina is somewhat higher than literature values for alkane-derivatized surfaces, which are typically around 110°.[29,30] This is undoubtedly due to the increased roughness of the microporous alumina surface.

Although over the concentration range $10^{-9}$ to $10^{-7}$ M there is some drop in membrane resistance with increasing DBS concentration, $R_m$ remains very large (>20 MΩ). However, over the DBS concentration range between $10^{-6}$ and $10^{-5}$ M, there is a precipitous, 4-order-of-magnitude, drop in $R_m$ (Figure 4). This drop signals the analyte-induced switching of the membrane from the off to the on states. The concentration of DBS that induces this off-to-on transition is well below the critical micelle concentration for DBS (1.1 mM).[31] The capacitance data also show the effect of this off/on transition. At concentrations of DBS below the transition, the membrane capacitance is extremely low (e.g., 0.46 nF/cm$^2$ of membrane surface area at a DBS concentration of $10^{-6}$ M) but jumps by 2 orders of magnitude when the membrane is switched to the on state (22 nF per cm$^2$ at [DBS] = $10^{-5}$ M).

**Transport Experiments.** The protocol used entailed spiking the electrolyte solutions as per the impedance experiments, allowing permeation to occur for 24 h, and then measuring the quantity of permeate ion transported to the permeate solution. The data obtained for $Ru(bpy)_3^{2+}$ transport are shown in Figure 4. At DBS concentrations below $10^{-6}$ M, there is no detectable $Ru(bpy)_3^{2+}$ in the permeate solution. It is important to emphasize that each permeation data point in Figure 4 corresponds to an additional 24 h of permeation time. Hence, by the time the DBS concentration was increased to $9 \times 10^{-7}$ M, the total permeation time was 5 days. The inability to detect $Ru(bpy)_3^{2+}$ in the permeate solution after 5 days of permeation shows that over the DBS concentration range 0 to ∼$10^{-6}$ M, the pores in the $C_{18}$ membrane are not wetted by water, making the rate of $Ru(bpy)_3^{2+}$ transport immeasurable small. These data again show that at DBS concentrations below $10^{-6}$ M, the membrane is in the off state.

At DBS concentrations above $10^{-6}$ M, $Ru(bpy)_3^{2+}$ transport is switched on, and flux increases with concentration of DBS for concentrations above this value. The impedance and transport data tell a consistent story about the effect of DBS on the $C_{18}$-derivatized membrane (Figure 4). At low DBS concentrations (<$10^{-6}$ M) where the membrane resistance is in the $10^7$ Ω range, $Ru(bpy)_3^{2+}$ is not transported. The sudden drop in $R_m$ at DBS concentrations above ∼$10^{-6}$ M is seen in the transport experiments as an abrupt switching on of $Ru(bpy)_3^{2+}$ transport across the membrane.

To understand the nature of this abrupt switch to the on state, we compared $Ru(bpy)_3^{2+}$ and $NDS^{2-}$ fluxes across bare (no $C_{18}$) alumina membranes with fluxes across $C_{18}$-modified membranes that had been exposed to $10^{-4}$ M DBS. The $Ru(bpy)_3^{2+}$ fluxes for the bare alumina membrane and for the $C_{18}$-modified membrane that had been exposed to $10^{-4}$ M DBS were found to be identical (data not shown). In the case of the bare membrane, the pores are flooded with water, and transport occurs by diffusion through these water-filled pores. The equivalence of the flux for the $C_{18}$-modified membrane that had been exposed to $10^{-4}$ M DBS clearly shows that the pores in this membrane are also flooded with water. The same results were obtained for the flux of the anionic permeate ion $NDS^{2-}$. An anion was studied to ensure that transport of the cationic $Ru(bpy)_3^{2+}$ was not being facilitated in some way by the anionic surfactant incorporated within the pores. Again, these data show that the transition from the off state to the on state occurs, because at DBS concentrations above $10^{-6}$ M, sufficient DBS has partitioned into the membrane that the pores spontaneously flood with water and electrolyte.

There is, however, one issue that remains unexplained. The $Ru(bpy)_3^{2+}$ and $NDS^{2-}$ flux data discussed above clearly show that exposure of the $C_{18}$−alumina membrane to $10^{-4}$ M DBS fully wets the pores, making them equivalent, in terms of this transport experiment, to the pores in the bare alumina membrane. This equivalence is not, however, observed in the membrane resistance experiment. That is, the resistance of the $C_{18}$−alumina membrane after exposure to $10^{-4}$ M DBS does not become equivalent to that of the bare alumina membrane. In fact, the $C_{18}$ membrane

(27) Ding, L.; Li, J.; Dong, S.; Wang, E. *J. Electroanal. Chem.* **1996**, *416*, 105−112.
(28) Ikematsu, M.; Iseki, M.; Sugiyama, S.; Mizukami, A. *Biosystems* **1995**, *35*, 123−128.
(29) Calistri-Yeh, M.; Kramer, E. J.; Sharma, R.; Zhao, W.; Rafailovich, M. H.; Sokolov, J.; Brock, J. D. *Langmuir* **1996**, *12*, 2747−2755.
(30) Pursch, M.; Vanderhart, D. L.; Sander, L. C.; Gu, X.; Nguyen, T.; Wise, S. A.; Gajewski, D. A. *J. Am. Chem. Soc.* **2000**, *122*, 6997−7011.
(31) Ohki, K.; Tokiwa, F. *J. Chem. Soc. Jpn. Chem. Ind. Chem.* **1970**, *91*, 534−539.

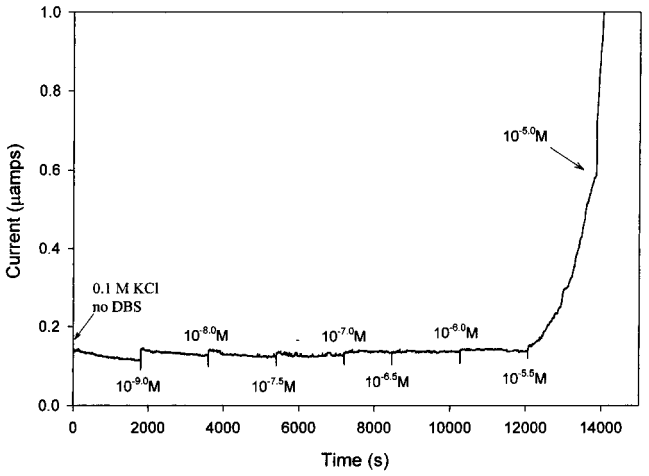


Figure 5. Ion current through a $C_{18}$-modified alumina membrane vs time. The contacting solution phases were spiked with the indicated concentrations of DBS at the indicated times. The electrolyte was 0.1 M KCl. A constant transmembrane potential of 1.5 V was applied.

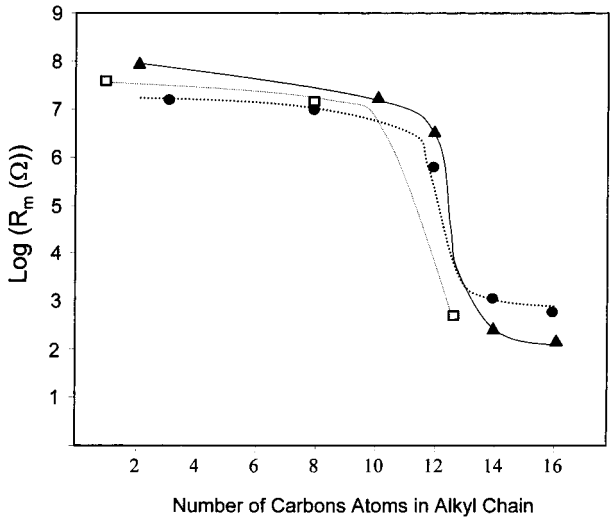


Figure 6. Plots of log membrane resistance for $C_{18}$-modified alumina membranes as a function of the carbon chain length of the surfactant exposed to the membrane. Prior to measurement, the membranes were soaked in 0.1 wt % surfactant solutions. □, Benzenesulfonate; ●, sulfonate; and ▲, trimethylammonium surfactant families.

resistance after exposure $10^{-4}$ M DBS remains two orders above the bare alumina resistance. One possible explanation for this observation is that the resistance measurement for the bare alumina membrane contains a component associated with ionic conductivity along the pore wall, and that when the membrane is treated with the $C_{18}$ silane, this component is lost.

**Measurements of Ion Current.** Although the transport experiments show that the analyte DBS can switch on ion (e.g., $Ru(bpy)_3^{2+}$ and $NDS^{2-}$) transport across the membrane, we also wanted to get a direct measure of the ion current. To do this, a constant transmembrane potential of 1.5 V was applied, and the resulting transmembrane ion current was measured. Figure 5 shows the measured ion current vs time data; at the indicated times, the electrolyte solutions were spiked to the indicated concentrations with DBS. The ion-current data show the same general trend as both the impedance and transport data: at concentrations below $\sim 10^{-6}$ M, the ion current is at a very low baseline value, and at concentrations above $\sim 10^{-6}$ M, the ion current abruptly switches on. In addition, the $10^{-5.5}$ M datum shows that the transition from the low-current to the high-current state occurs very abruptly.

Both the impedance and ion-current data show that when the membrane is in the off state, some small baseline current does flow across the membrane. It is important to note that the resistance values for the off state obtained by the impedance and ion-current measurements are essentially identical. As shown in Figure 4, the impedance measurement yields a value of $\sim 10^7$ Ω. The ion-current in the off state is $\sim 1.5 \times 10^{-7}$ A, which for a 1.5 V transmembrane potential yields a membrane resistance of $\sim 10^7$ Ω. The issue left to resolve, however, is what is supporting this baseline ion current when the membrane is in the off state? At this point, we cannot say other than to suggest that this current results from some surface conduction process that occurs along the pore walls when the pores are devoid of water. In the absence of DBS, this surface conduction process may involve residual surface hydroxyl sites. The impedance data (Figure 4) indicate that in the presence of DBS, the surfactant itself is involved in the conduction process.

**Effect of Alkyl Chain Length and Nature of the Surfactant Headgroup.** The above data show that partitioning of the analyte DBS into the membrane is responsible for the transition to the on state. It seems likely that this partitioning process is driven by the hydrophobic effect. To prove this point, $C_{18}$-modified alumina membranes were exposed to 0.1 wt % solutions of various alkyl sulfonate, alkyl benzene sulfonate, and trimethyl alkylammonium surfactants. (0.1 wt % corresponds to 8.1 mM for the smallest surfactant and 2.8 mM for the largest.) The membranes were then rinsed, and the impedances were determined in 0.1 M KCl that was devoid of surfactant. Figure 6 shows plots of log membrane resistance vs number of carbon atoms in the alkyl side chain for all of the surfactants investigated. These data show that in order for a surfactant to switch the membrane to the on state, the alkyl chain must be above some minimum length. For the alkyl benzene sulfonates, a 12-carbon chain is required. For the alkyl sulfonates and alkylammoniums, the alkyl group must be at least 14 carbons long (Figure 6).

These data clearly show that the hydrophobic effect is responsible for driving the surfactant into the $C_{18}$-modified membrane. The difference between the alkyl benzene sulfonates and the other two classes of surfactants reflects the added contribution of the benzene group to the hydrophobicity. With the added benzene group, a 12-carbon alkyl chain can switch the membrane to the on state; without the benzene group, a 14-carbon chain is needed (Figure 6). The data in Figure 6 also show that for the long-chain surfactants, the adsorption of the surfactant to the membrane is essentially irreversible if the membrane is exposed to aqueous solution. However, we have found that the surfactant can be removed from the membrane by rinsing with ethanol. After the ethanol rinse, the membrane resistance returns to values equivalent to the off state obtained prior to exposure to surfactant.

**Detection of Drug Molecules.** To further explore the role of the hydrophobic effect in driving the analyte species into the $C_{18}$-derivatized alumina membrane, we investigated the effect of

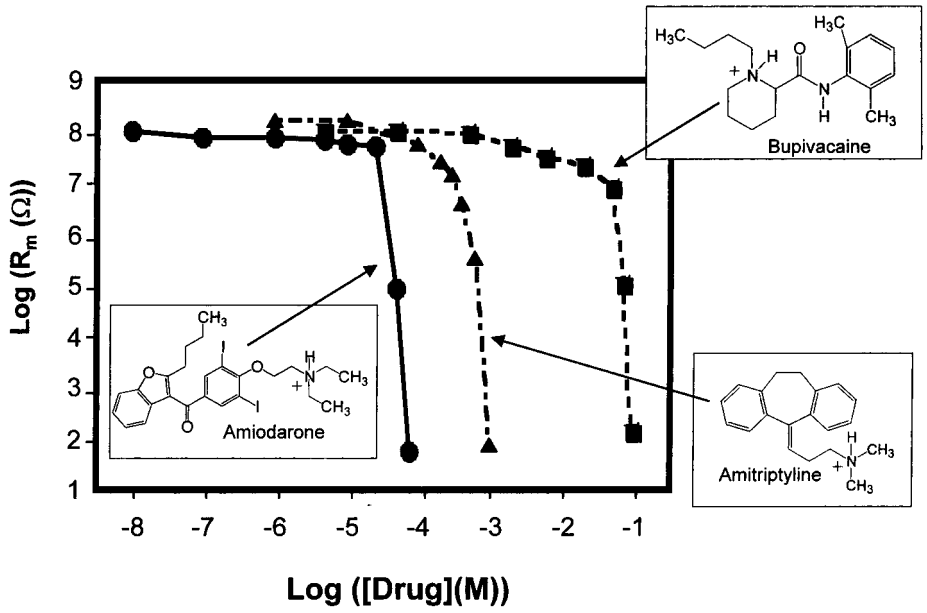


Figure 7. Plots of log membrane resistance vs log[drug] for the indicated drugs and a $C_{18}$-modified alumina membrane.

hydrophobic cationic drug molecules on the membrane resistance. The molecules and their molecular weights are amiodarone (645 g $mol^{-1}$), amitriptyline (278 g $mol^{-1}$), and bupivacaine (288 g $mol^{-1}$) (Figure 7). Because its molecular weight is more than double those of the other drugs and because it contains very hydrophobic iodo substituents, amiodarone is by far the most hydrophobic of these molecules. If the hydrophobic effect is responsible for driving molecules into the $C_{18}$-derivatized membrane, then the transition from the off to the on state would occur at lowest concentrations for amiodarone, and this is what is observed experimentally (Figure 7). There is only a 3% difference in the molecular weights of amitriptyline and bupivacaine; however, bupivacaine presents two additional opportunities for hydrogen bonding with water: the lone pairs on the carbonyl group and the lone pair of the nonprotonated nitrogen. For this reason, bupivacaine is much more hydrophilic, and it would be expected to be the most poorly detected of the three drugs; Figure 7 shows that this is also observed experimentally.

**Switching the Membrane in Response to Solution pH.** We have also investigated the effect of solution pH on the resistance of a membrane that was derivatized with $-Si-(CH_2)_3NHCO-(CH_2)_{20}-COOH$. This carboxylic acid was used because such long-chain aliphatic acids are insoluble in water in their protonated forms. We reasoned that this hydrophobicity would render the pore nonwater-wetted at low solution pH values. In agreement with this supposition, the resistance of the $-Si-(CH_2)_3NHCO-(CH_2)_{20}-COOH$-deravitized membrane is $10^5$ Ω when exposed to solutions having pH values in the range of 5.5 to 7.0. This signifies the off state of the membrane. That the resistance of the off state for this membrane is lower than that for the $C_{18}$-derivatized membrane is not surprising, because the 18-carbon alkyl chain is certainly more hydrophobic than the $-(CH_2)_3NHCO-(CH_2)_{20}-COOH$ chain. At pH 8.0, the membrane resistance drops slightly to $10^{4.4}$ Ω. Above pH 8, there is a large (>4-order-of-magnitude) drop in membrane resistance, signifying the transition to the on state.

The transition to the on state is associated with the deprotonation of the carboxylic acid group. This is a reversible effect; the fully deprotonated membrane obtained after exposure to pH 10 buffer can be rinsed and dried and then reexposed to pH 5.5 buffer to regenerate the off state of the membrane. Finally, if it is assumed that the surface-bound long-chain carboxylic acid has a typical aqueous-solution-phase $K_a$ ($\sim 10^{-5}$), then the transition to the on state occurs when 99.9% of the −COOH groups have been deprotonated. This is, however, only an approximation, because the very hydrophobic environment within the silane-modified pores may substantially change the $K_a$ relative to the solution value. For example, surface p$K_a$ values as much as 2−3 log units larger than corresponding solution values have been observed.[32,33] This effective weakening of the surface-bound acid could explain why the on transition is observed at pH 8.

**The Effect of Pore Density and Pore Diameter on Analyte Detection.** Au nanotube membranes that were rendered hydrophobic by chemisorbing octadecyl thiol[4] were used to explore these issues. These membranes contained ∼2-nm-i.d. Au nanotubes and had a total porosity of only $2 \times 10^{-3}$%. This may be contrasted to the alumina membranes, which contain pores that are 2 orders of magnitude larger in diameter and are ∼30% porous. In a study analogous to Figure 4, we examined the resistance of these membranes with increasing concentration of DBS. An abrupt transition from a very high resistance ($10^9$ Ω) off state to a 4-order-of-magnitude lower-resistance on state is observed over essentially the same concentration range as is observed for the $C_{18}$-derivatized alumina membranes.

These results show that for membranes containing either $C_{18}$-modified alumina micropores or $C_{18}$-modified Au nanotubes, the concentration of DBS that induces the transition form the off to the on state does not depend on porosity or pore/tube diameter. Although at first glance this may seem surprising, it is important to point out that changing the porosity or pore/nanotube diameter

(32) Kane, V.; Mulvaney, P. *Langmuir* **1998**, *14*, 3303−3311.
(33) Hu, K.; Bard, A. J. *Langmuir* **1997**, *13*, 5114−5119.

in reality changes only the surface area of $C_{18}$ groups available for the adsorption of analyte; that is, the low-porosity Au nanotube membranes have a lower surface area available for analyte adsorption than do the alumina membranes. This situation can be modeled by assuming that the analyte is adsorbed onto the $C_{18}$-modified surfaces via a Langmuir isotherm and that a certain critical fraction ($\Theta_c$) of the surface must be covered with analyte in order to flood the pores with electrolyte. $\Theta_c$ is related to the equilibrium constant for the adsorption reaction ($\beta$) and the activity of DBS in the solution phase ($a_{DBS}$) via[34]

$$\Theta_c = (\beta a_{DBS})/(1 + \beta a_{DBS}) \quad (1)$$

Equation 1 shows that $\Theta_c$ depends only on the value of the equilibrium constant (the same for both membranes, since both contain $C_{18}$ alkyl groups) and the activity of surfactant in solution. Because surface area does not enter into the equation, the concentration of DBS required to switch the membrane to the on state should be independent of membrane porosity and pore diameter, and this is what is observed experimentally.

## CONCLUSIONS

We have shown that synthetic micropore and nanotube membranes can mimic the function of ligand-gated ion channels; that is, they can be switched from an off state to an on state in response to the presence of a chemical stimulus. The off state was obtained by making the membranes hydrophobic, and the on state was obtained by introducing ions and electrolyte into the membrane. Ions were introduced by either partitioning a hydrophobic ionic species (e.g., a drug or a surfactant) into the membrane or by deprotonation of a surface-bound hydrophobic carboxylic acid. In the partitioning case, the concentration of surfactant required to switch a $C_{18}$-derivatized membrane to the on state does not depend on membrane pore diameter or porosity. It does, however, depend on the hydrophobicity of the analyte, with more-hydrophobic analytes yielding the on state at lower concentrations. In this regard, these sensors are qualitatively very similar to ion-selective electrodes developed for hydrophobic cations that were based on a hydrophobic anion exchange reagent.[35,36] In both cases, the sensor could be useful in an environment in which only one hydrophobic ionic analyte is present; that is, all other ions in the analyte solution are hydrophilic. The pH-sensing device might prove useful as a biosensor if coupled to an enzymatic process that produces a base. An example would be urease-catalyzed hydrolysis of urea. We are currently investigating this possibility.


## ACKNOWLEDGMENT

Aspects of this work were supported by the Office of Naval Research and the National Science Foundation.

Received for review January 11, 2002. Accepted March 15, 2002.

AC020024J



(34) Bard, A. J.; Faulkner, L. R. *Electrochemical Methods*; John Wiley and Sons: New York, 1980; pp 516−518.
(35) Martin, C. R.; Freiser, H. *Anal. Chem.* **1980**, *52*, 562−564.
(36) Martin, C. R.; Freiser, H. *Anal. Chem.* **1980**, *52*, 1772−1774.